IEEE Access
Multidisciplinary | Rapid Review | Open Access Journal

Received January 28, 2019, accepted February 7, 2019, date of publication February 12, 2019, date of current version March 29, 2019.

Digital Object Identifier 10.1109/ACCESS.2019.2898925

Adaptive Neural Funnel Control for Nonlinear Two-Inertia Servo Mechanisms With Backlash

SHUBO WANG[1], (Member, IEEE), HAISHENG YU[1], JINPENG YU[1], AND XUEHUI GAO[2], (Member, IEEE)

[1]School of Automation, Qingdao University, Qingdao 266071, China
[2]Department of Mechanical and Electrical Engineering, Shandong University of Science and Technology, Tai'an 2701019, China

Corresponding author: Shubo Wang (wangshubo1130@126.com)

This work was supported in part by the National Natural Science Foundation of China under Grant 61803216, Grant 61573203, and Grant 61573204, and in part by the Natural Science Foundation of Shandong Province under Grant ZR2018BF022 and Grant ZR2017MF048.

ABSTRACT This paper proposes a modified adaptive neural control algorithm with a funnel function for nonlinear two-inertia servomechanisms with backlash and external disturbance. A continuous tracking differentiator is employed to replace the first-order filter in the traditional dynamic surface control design. A novel funnel function is employed and used in control design to improve the control performance. Then, an adaptive neural dynamic surface controller based on funnel control is presented to guarantee the tracking performance of two-inertia servomechanisms. In addition, the unknown dynamics, including backlash, nonlinear friction, and external disturbance, are approximated by using the echo state neural network and compensated online. The comparative experimental results validate the effectiveness of the developed control algorithm based on a two-inertia servo mechanism.

INDEX TERMS Adaptive control, neural network, servo mechanisms, prescribed performance control.

I. INTRODUCTION

High performance servo drive systems have been of great importance in practical engineering applications [1]–[7], e.g., robot-arm drives, wind power generation, and electric vehicle. However, there exist some nonlinearities such as nonlinear friction, backlash and external disturbances that can reduce the control performance. Among these nonlinearities, the backlash appearing in the transmission device which degrades the transmission performance. To reduce the effect of the backlash, some advanced control methods have been developed, e.g., sliding mode control [8], [9], robust control [10] and adaptive control [11]. In addition, artificial intelligence technologies (e.g., neural network [12]–[17] and fuzzy logic control [18]–[21]) have also been utilized to compensate the nonlinearities owing to their nonlinear approximation and learning abilities.

Recently, backstepping technique is an effect way to cope with the nonlinearities of the control systems. In the traditional backstepping design procedure [22]–[24], there exists ''explosion of complexity'' in virtual controller designed at each step needs repeated differentiation. To remedy this drawback, dynamic surface control (DSC) technique was proposed in [25]. The DSC has been successfully applied to control nonlinear systems. For example, a composite neural DSC method was developed for nonlinear system with uncertainties [26]. In [27]a, the neural network based adaptive DSC was designed for autonomous surface vehicles with uncertain dynamics. An adaptive robust DSC was developed for servo mechanisms with electrical dynamics and unmeasurable states to improve the control performance [28]. An adaptive fuzzy DSC was proposed for nonlinear pure-feedback systems [29]. An adaptive neural DSC for servo mechanisms with unknown dead-zone was proposed in [30]. A novel adaptive DSC with error constraint was developed for MIMO nonlinear systems [31]. These control methods have improved the control performance from different aspects.

However, the transient and stead-state performance of the control systems are not be guaranteed in industrial applications. To overcome this issue, the prescribed performance control (PPC) was proposed to guarantee the convergence rate and the maximum overshoot of the tracking error in [32]. The idea is that both the transient and steady-state control performance can be analytically examined and prescribed by introducing a prescribed performance function (PPF) and a coordinate error transform. This method has been successfully applied in some control systems, such as

The associate editor coordinating the review of this manuscript and approving it for publication was Yan-Jun Liu.

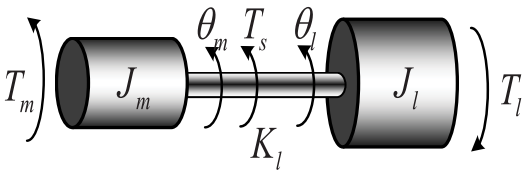

FIGURE 1. System model of two-inertia drive system.

motor drive system [33], spacecraft system [34], manipulators control system [35], surface vessel [36], and vehicle suspensions [37]. Nevertheless, the transformation error need to calculate the partial differential that may cause the stability problem. In addition, funnel control (FC) [38] has also been used to guarantee prescribed transient response. Until now, the applications of the FC control has been used in some fields such that motor control system [39], motion control system [40], and robotic system [41].

This paper presents an adaptive neural funnel control for two-inertia servo mechanisms with backlash. A continuous tracking differentiator (CTD) is employed to replace the first-order filter in conventional DSC design, a modified DSC is proposed to achieve the load tracking. A novel funnel variable is defined and incorporated into control design. The unknown dynamics are approximated by using echo state neural network where the weights are all updated online. By using Lyapunov stability theory, all the signals of the closed-loop control system are the semiglobally uniformly ultimately bounded (SGUUB). Comparative experimental results validate the effectiveness of the developed control algorithm based on a two-inertia servo mechanism.

The main contributions can be listed as follows.

1) A CTD is adopted to replace the first-order filter in virtual intermediate control signal of conventional DSC design to improve the filter performance.

2) To improve the convergence rate and overshoot of the tracking error, a modified funnel function is incorporated into DSC design for two-inertia servo mechanisms.

3) The unknown dynamics are approximated by using echo state neural network where the weights are all updated online.

This paper is organized as follows. Section II presents the problem statement. The control design is shown in Section III. Experimental verification based on a servo system is shown in Section IV. Section V provides some conclusions.

II. PROBLEM STATEMENT AND PRELIMINARIES

A. SYSTEM MODEL

This paper considers two-inertia system, which is comprised of a servo motor connected a load via a transmission gear (See Fig. 1). Then, the mechanical model of the two-inertia system, including the backlash is described as follows:

$$\begin{cases} J_m\ddot{\theta}_m + b_m\dot{\theta}_m + T_s = T_m \\ J_l\ddot{\theta}_l + b_l\dot{\theta}_l - T_s = 0 \end{cases} \tag{1}$$

where J_m and J_l are, respectively, the motor inertia and load inertia; θ_m, and $\dot{\theta}_m$ denote the motor angular position and angular speed; θ_l, and $\dot{\theta}_l$ represent the load angular position and load speed; b_m and b_l are the friction coefficients, T_s represents the transmission torque between the motor and the load; T_m is the input torque.

In this paper, the transmission torque is described by using a continuous differentiable function which is defined as

$$T_s = kf(\Delta\theta) = k\left(\Delta\theta - \alpha\left(\frac{2}{1+e^{-r\Delta\theta}} - 1\right)\right) \tag{2}$$

where r is a positive constant, $\Delta\theta = \theta_m - \theta_l$, k denotes stiffness coefficient, and α is the backlash width.

Select the state variable as $x = [x_1 \;\; x_2 \;\; x_3 \;\; x_4]^T = [\theta_l \;\; \dot{\theta}_l \;\; \theta_m \;\; \dot{\theta}_m]^T$, then the system model (1) can be written as

$$\begin{cases} \dot{x}_1 = x_2 \\ \dot{x}_2 = \dfrac{b_l}{J_l}x_4 + \dfrac{1}{J_l}k\left((x_1 - x_3) - \alpha\left(\dfrac{2}{1+e^{-r(x_1-x_3)}} - 1\right)\right) \\ \dot{x}_3 = x_4 \\ \dot{x}_4 = -\dfrac{b_m}{J_m}x_2 + \dfrac{1}{J_m}u \\ \qquad -\dfrac{1}{J_m}k\left((x_1 - x_3) - \alpha\left(\dfrac{2}{1+e^{-r(x_1-x_3)}} - 1\right)\right) \end{cases} \tag{3}$$

Assumption 1: The reference signal x_d and its first and second time derivative $\dot{x}_d$ and $\ddot{x}_d$ are continuous and bounded.

The aim of this paper is to present an adaptive control for servo mechanism (1) with backlash to make the output position x_1 to tracking the reference x_d, and the unknown backlash is approximated by using ESN and compensated in control design.

B. ESN APPROXIMATION

ESN has been successfully utilized to approximate the nonlinearity due to their approximation and learning abilities. It comprised of three parts, as depicted in Fig.2: 1) K input neurons, 2) a reservoir layer with N reservoir neurons, and 3) output layer with L output neurons. The continuous-time state of reservoir neurons is defined as

$$\begin{aligned} \dot{X} &= C(-aX + f(W^{in}u + WX + W^{back}y)) \\ y &= G(W_0^T X) \end{aligned} \tag{4}$$

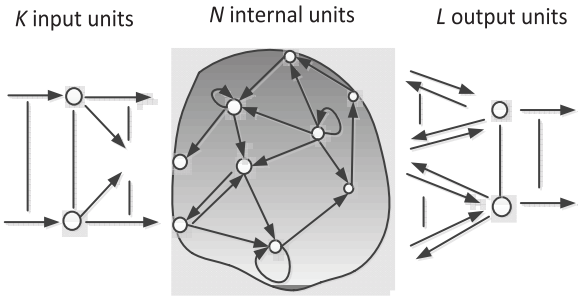

FIGURE 2. Basic architecture of ESN.

where X denotes reservoir neuron state, $C > 0$ is a time constant, a represents the leaking decay rate. $W^{in} \in R^{N\times K}$, $W \in R^{N\times N}$ and $W^{out} \in R^{N\times L}$ denote the input weight matrix, the reservoir weight matrix, and the feedback weight matrix, respectively. The ESN can be used to approximate any continuous function $f(x)$ over a compact domain $\Omega \in R^m$.

The function $f(x)$ is expressed as

$$f(x) = W^*\Phi(x) + \varepsilon^* \quad \forall x \in \Omega \subset R^m \tag{5}$$

where ε^* is the approximation error, and $|\varepsilon^*| \leq \varepsilon_m$, W^* represents the ideal value of ESN weights. Therefore

$$W^* = \arg\min_{W\in R^L} \left\{ \sup_{x\in\Omega} |f(x) - W^{*T}X(x)| \right\} \tag{6}$$

C. FUNNEL CONTROL

Funnel-control (FC), developed by Ilchmann *et al.* [38], is new control strategy which is based the high-gain concepts and adopts an adjustable proportional gain $\tau(\cdot)$ to control and stabilize all systems of class S [38].

The control input can be expressed as

$$u(t) = \tau(F_\varphi(t), \psi(t), \|e(t)\|) \cdot e(t) \tag{7}$$

where $\psi(t)$ is scaling factor. The distance $d_v(t)$ is defined as

$$d_v(t) = F_\varphi(t) - \|e(t)\| \tag{8}$$

where $e(t)$ is the tracking error, which is defined as

$$e(t) = x_d - x(t) \tag{9}$$

where x_d and $x(t)$ denote the reference signal and output.

Thus the funnel itself is defined as the set

$$F_\varphi := \{(t, e) \in R \times R^n | \varphi(t) \cdot \|e(t)\| < 1\} \tag{10}$$

Based on [38], this boundary (See Fig.3) can be described by

$$F_\varphi(t) = \varphi_0 \cdot \exp(-at) + \varphi_\infty \tag{11}$$

where φ_0, φ_∞, a are design parameters.

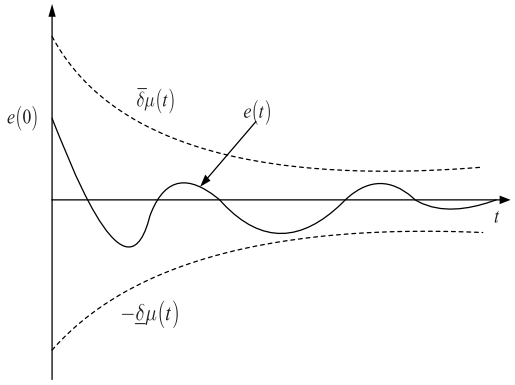

FIGURE 3. Funnel-control block diagram [38].

The gain $\tau(\cdot)$ [38] can be adjusted by

$$\tau(F_\varphi(t), \psi(t), \|e(t)\|) = \frac{\psi(t)}{F_\varphi(t) - \|e(t)\|} \tag{12}$$

to ensure that the error $e(t)$ evolves inside the funnel $F_\varphi(t)$. Therefore, the gain $\tau(t)$ increases, the error $e(t)$ draws close to the boundary $F_\varphi(t)$; if the gain $\tau(t)$ decreases, the error $e(t)$ becomes small.

This paper defines a modified funnel function as

$$z(t) = \frac{e(t)}{F_\varphi(t) - \|e(t)\|} \tag{13}$$

where the boundary $F_\varphi(t)$ satisfies the condition given in (10).

III. CONTROLLER DESIGN

In this part, the funnel function is utilized to design DSC for servo mechanisms. The controller design steps are given in the follows. The overall control structure of the closed-loop system is depicted in Fig.4.

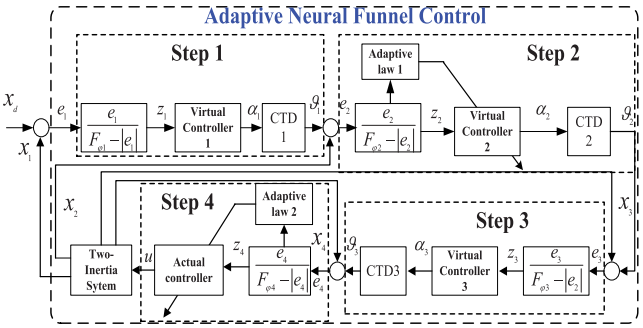

FIGURE 4. Structure of the proposed controller for two-inertia servo system.

A. CONTINUOUS TRACKING DIFFERENTIATOR, (CTD)

The CTD [42] can be designed as

$$\begin{cases} \dot{\vartheta} = \upsilon - \lambda_1|\vartheta - x_r|^{(m+1)/2}\mathrm{sgn}(\vartheta - x_r) - \lambda_2(\vartheta - x_r) \\ \dot{\upsilon} = -\lambda_3|\vartheta - x_r|\mathrm{sgn}(\vartheta - x_r) - \lambda_4(\vartheta - x_r) \end{cases} \tag{14}$$

where $\lambda_i (i = 1, ..., 4)$ and m are the positive constants. x_r denotes the input signal of the CTD.

Lemma 1: If the input signal χ_i is the bounded and differentiable, there exist constants $\lambda_i > 0$ and $0 < m < 1$ such that the following inequalities hold in finite-time (FT).

$$\begin{aligned} |\vartheta - x_r| &\leq \ell_1 \\ |\upsilon - \dot{x}_r| &\leq \ell_2 \end{aligned} \tag{15}$$

where ℓ_1, and ℓ_2 are positive constants which depend on design parameters λ_i and m.

B. CONTROLLER DESIGN

Step 1: Define the tracking error as

$$e_1 = x_1 - x_d \tag{16}$$

where x_d is the reference signal. Based on (13), the funnel variable z_1 is defined as

$$z_1 = \frac{e_1}{F_{\varphi 1} - |e_1|} \tag{17}$$

The time derivative of z_1 is

$$\begin{aligned}\dot{z}_1 &= \frac{1}{(F_{\varphi_1} - |e_1|)^2}\left[\dot{z}_1(F_{\varphi_1} - |e_1|) - e_1(\dot{F}_{\varphi_1} - |\dot{e}_1|)\right] \\ &= \xi_1\left[x_2 - (\dot{F}_{\varphi_1} - |\dot{e}_1|)z_1 - \dot{x}_d\right]\end{aligned} \tag{18}$$

where $\xi_1 = \frac{1}{F_{\varphi_1} - |e_1|}$.

Let x_d through a CTD, one has

$$\begin{cases}\dot{\vartheta}_1 = \upsilon_1 - \lambda_{11}|\vartheta - x_r|^{(m_1+1)/2}\mathrm{sgn}(\vartheta_1 - x_d) \\ \quad -\lambda_{21}(\vartheta_1 - x_d) \\ \dot{\upsilon}_1 = -\lambda_{31}|\vartheta_1 - x_d|\mathrm{sgn}(\vartheta_1 - x_d) - \lambda_{41}(\vartheta_1 - x_d)\end{cases} \tag{19}$$

where $\lambda_{i1}(i = 1, 2, 3, 4)$ and m_1 are design parameters. ϑ_1 represents the filter signal of the x_d.

The virtual control signal α_1 is designed as

$$\alpha_1 = -k_1\xi_1 z_1 + (\dot{F}_{\varphi_1} - |\dot{e}_1|)z_1 + \vartheta_1 \tag{20}$$

where k_1 is the design parameter.

Step 2: Define the second error surface $e_2 = x_2 - \alpha_1$. Based on the error transformation function (13), we can obtain that

$$z_2(t) = \frac{e_2(t)}{F_{\varphi 2} - |e_2(t)|} \tag{21}$$

The time derivative of $z_2(t)$ is

$$\begin{aligned}\dot{z}_2 &= \frac{1}{(F_{\varphi_2} - |e_2|)^2}\left[\dot{z}_2(F_{\varphi_2} - |e_2|) - e_1(\dot{F}_{\varphi_2} - |\dot{e}_2|)\right] \\ &= \xi_2\left[\dot{x}_2 - (\dot{F}_{\varphi_2} - |\dot{e}_2|)z_2 - \dot{\alpha}_1\right] \\ &= \xi_2\Big[-\frac{b_l}{J_l}x_2 + \frac{1}{J_l}(x_1 - x_3) + W_1\Phi(x) \\ &\quad - (\dot{F}_{\varphi_2} - |\dot{e}_2|)z_2 - \dot{\alpha}_1\Big]\end{aligned} \tag{22}$$

where $\xi_2 = \frac{1}{F_{\varphi_2} - |e_2|}$.

Let α_2 through the TD, we have

$$\begin{cases}\dot{\vartheta}_2 = \upsilon_2 - \lambda_{12}|\vartheta - \alpha_1|^{(m_2+1)/2}\mathrm{sgn}(\vartheta_2 - \alpha_1) \\ \quad -\lambda_{22}(\vartheta_1 - x_d) \\ \dot{\upsilon}_2 = -\lambda_{32}|\vartheta_1 - \alpha_1|\mathrm{sgn}(\vartheta_2 - \alpha_1) - \lambda_{42}(\vartheta_2 - x_d)\end{cases} \tag{23}$$

where $\lambda_{i2}(i = 1, 2, 3, 4)$ and m_2 are the design parameters. ϑ_2 is the filter signal of the virtual control signal α_1.

A virtual control α_2 is given as

$$\begin{aligned}\alpha_2 = J_l(&-k_2\xi_2 z_2 + (\dot{F}_{\varphi_2} - |\dot{e}_2|)z_2 \\ &+ \vartheta_2) + b_l(x_2 - x_1) - \hat{W}_1\Phi(x)\end{aligned} \tag{24}$$

and

$$\dot{\hat{W}}_1 = \Gamma_1[z_2\xi_2\Phi(x) - \sigma_1\hat{W}_1] \tag{25}$$

where k_2, Γ and σ_1 are the design parameters.

Step 3: Define the third tracking error $e_3 = x_3 - \alpha_2$. Then, the funnel variable $z_3(t)$ is defined as

$$z_3 = \frac{e_3}{F_{\varphi 3} - |e_3|} \tag{26}$$

The time derivative of z_3 is

$$\begin{aligned}\dot{z}_3 &= \frac{1}{(F_{\varphi_3} - |e_3|)^2}\left[\dot{z}_3(F_{\varphi_3} - |e_3|) - e_3(\dot{F}_{\varphi_3} - |\dot{e}_3|)\right] \\ &= \xi_3\left[x_4 - (\dot{F}_{\varphi_3} - |\dot{e}_3|)z_3 - \dot{\alpha}_2\right]\end{aligned} \tag{27}$$

where $\xi_3 = \frac{1}{F_{\varphi_3} - |e_3|}$

Let α_3 through the TD, we have

$$\begin{cases}\dot{\vartheta}_3 = \upsilon_3 - \lambda_{13}|\vartheta_3 - \alpha_2|^{(m_3+1)/2}\mathrm{sgn}(\vartheta_3 - \alpha_2) \\ \quad -\lambda_{23}(\vartheta_3 - \alpha_2) \\ \dot{\upsilon}_3 = -\lambda_{33}|\vartheta_3 - \alpha_2|\mathrm{sgn}(\vartheta_3 - \alpha_2) - \lambda_{43}(\vartheta_3 - \alpha_2)\end{cases} \tag{28}$$

where $\lambda_{i3}(i = 1, 2, 3, 4)$ and m_3 are the design parameters. ϑ_3 is the filter signal of the virtual control signal α_2.

A virtual control α_3 is given as

$$\alpha_3 = -k_3\xi_3 z_3 + (\dot{F}_{\varphi_3} - |\dot{e}_3|)z_3 + \vartheta_3 \tag{29}$$

where k_3 is the design parameter.

Step 4: Define the last error surface $e_4 = x_4 - \alpha_3$, then, the funnel variable is given as

$$z_4 = \frac{e_4}{F_{\varphi 4} - |e_4|} \tag{30}$$

The time derivative of z_4 is

$$\begin{aligned}\dot{z}_4 &= \frac{1}{(F_{\varphi_4} - |e_4|)^2}\left[\dot{z}_4(F_{\varphi_4} - |e_4|) - e_4(\dot{F}_{\varphi_4} - |\dot{e}_4|)\right] \\ &= \xi_4\left[\dot{x}_4 - (\dot{F}_{\varphi_4} - |\dot{e}_4|)z_4 - \dot{\alpha}_3\right] \\ &= \xi_4\Big[-\frac{b_m}{J_m}x_2 + \frac{1}{J_m}u - \frac{1}{J_m}k(x_1 - x_3) - W_2\Phi(x) \\ &\quad - (\dot{F}_{\varphi_4} - |\dot{e}_4|)z_4 - \dot{\alpha}_3\Big]\end{aligned} \tag{31}$$

Let α_3 passes through the TD as

$$\begin{cases}\dot{\vartheta}_4 = \upsilon_4 - \lambda_{14}|\vartheta_4 - \alpha_3|^{(m_4+1)/2}\mathrm{sgn}(\vartheta_4 - \alpha_3) \\ \quad -\lambda_{24}(\vartheta_4 - \alpha_3) \\ \dot{\upsilon}_4 = -\lambda_{34}|\vartheta_4 - \alpha_3|\mathrm{sgn}(\vartheta_4 - \alpha_3) - \lambda_{44}(\vartheta_4 - \alpha_3)\end{cases} \tag{32}$$

where $\lambda_{i4}(i = 1, 2, 3, 4)$ and m_4 are the design parameters. ϑ_4 is the filter signal of the virtual control α_3.

The true control action u is designed as

$$\begin{aligned}u = -k_4\xi_4 z_4 + \frac{b_m}{J_m}x_2 + \frac{1}{J_m}k(x_1 - x_3) + \hat{W}_2\Phi(x) \\ + (\dot{F}_{\varphi_4} - |\dot{e}_4|)z_4 + \vartheta_4\end{aligned} \tag{33}$$

and

$$\dot{\hat{W}}_2 = \Gamma_2[z_4\xi_4\Phi(x) - \sigma_2\hat{W}_2] \tag{34}$$

C. STABILITY ANALYSIS

Theorem 1: Consider the two-inertia system (1) with backlash model (2). If the visual control signals are designed as (20), (24) and (29), and the actual control action (33), the load output position x_1 can track desired trajectory x_d and all the signals are the semi-globally uniformly ultimately bounded (SGUUB).

Proof: Define a Lyapunov function as

$$V = \frac{1}{2}\sum_{i=1}^{4} z_i^2 + \frac{1}{2}\sum_{j=1}^{2} \tilde{W}_j^T \Gamma_j^{-1} \tilde{W}_j^T \tag{35}$$

The time derivative of V is

$$\begin{aligned}\dot{V} &= \sum_{i=1}^{4} z_i \dot{z}_i + \sum_{j=1}^{2} \tilde{W}_j^T \Gamma_j^{-1} \dot{\tilde{W}}_j^T \\ &= z_1\xi_1\big[\alpha_1 + e_1 - (\dot{F}_{\varphi_1} - |\dot{e}_1|)z_1 - \dot{x}_d\big] \\ &\quad + z_2\xi_2\big[-\frac{b_l}{J_l}x_2 + \frac{1}{J_l}(x_1 - \alpha_2 - e_2) + W_1\Phi(x) - (\dot{F}_{\varphi_2} \\ &\quad - |\dot{e}_2|)z_2 - \dot{\alpha}_1\big] + z_3\xi_3\big[\alpha_3 + e_3 - (\dot{F}_{\varphi_3} - |\dot{e}_3|)z_3 - \dot{\alpha}_2\big] \\ &\quad + z_4\xi_4\big[-\frac{b_m}{J_m}x_2 + \frac{1}{J_m}u - \frac{1}{J_m}k(x_1 - x_3) - W_2\Phi(x) \\ &\quad - (\dot{F}_{\varphi_4} - |\dot{e}_4|)z_4 - \dot{\alpha}_3\big] + \tilde{W}_1 z_2\xi_2\Phi(x) - \sigma_1\tilde{W}_1\hat{W}_1 \\ &\quad + \tilde{W}_2 z_4\xi_4\Phi(x) - \sigma_2\tilde{W}_2\hat{W}_2 \end{aligned} \tag{36}$$

Substituting the visual control (20), (24), (29) and actual control action (33) into (36), we can obtain that

$$\begin{aligned}\dot{V} &= -k_1\xi_1 z_1^2 + z_1\xi_1 e_1 - k_2\xi_2 z_2^2 + z_2\xi_2 e_2 - k_3\xi_3 z_3^2 \\ &\quad + z_3\xi_3 e_3 - z_2\xi_2\tilde{W}_1\Phi(x) - z_4\xi_4\tilde{W}_2\Phi(x) + \tilde{W}_1 z_2\xi_2\Phi(x) \\ &\quad - \sigma_1\tilde{W}_1\hat{W}_1 + \tilde{W}_2 z_4\xi_4\Phi(x) - \sigma_2\tilde{W}_2\hat{W}_2 \\ &= -k_1\xi_1^2 z_1^2 + z_1\xi_1 e_1 - k_2\xi_2^2 z_2^2 + z_2\xi_2 e_2 - k_3\xi_3^2 z_3^2 \\ &\quad + z_3\xi_3 e_3 - \sigma_1\tilde{W}_1\hat{W}_1 - \sigma_2\tilde{W}_2\hat{W}_2 \end{aligned} \tag{37}$$

Using Young's inequality yields

$$\begin{aligned} z_i\xi_i e_i &\le \frac{1}{2}z_i^2\xi_i^2 + \frac{1}{2}e_i^2, \quad i = 1, 2, 3 \\ -\sigma_j\tilde{W}_j\hat{W}_j &\le -\frac{\sigma_j\|\tilde{W}_j^2\|}{2} + \frac{\sigma_j\|W_j\|}{2}, \quad j = 1, 2 \end{aligned} \tag{38}$$

Substituting (38) into (37), one has

$$\begin{aligned}\dot{V} &= -(k_1 - \frac{1}{2})\xi_1^2 z_1^2 - (k_2 - \frac{1}{2})\xi_2^2 z_2^2 - (k_3 - \frac{1}{2})\xi_3^2 z_3^2 \\ &\quad - k_4\xi_4^2 z_4^2 - \sum_{j=1}^{2}\frac{\sigma_j\|\tilde{W}_j^2\|}{2} + \sum_{j=1}^{2}\frac{\sigma_j\|W_j\|}{2} \\ &\le -2\rho V + \delta \end{aligned} \tag{39}$$

where $\rho = \min\{k_1 - \frac{1}{2}, k_2 - \frac{1}{2}, k_3 - \frac{1}{2}, k_4, \frac{\sigma_j\|\tilde{W}_j^2\|}{2}\}$ and $\delta = \frac{\sigma_j\|W_j\|}{2}$.

By integrating both sides of (39), we have

$$0 \le V(t) \le \frac{\delta}{2\rho} + \big(V(0) - \frac{\delta}{2\rho}\big)e^{-2\rho t} \tag{40}$$

From (40), one can conclude that all the signals of the closed-loop are SGUUB.

In engineering applications, the parameter tuning rules of the proposed control algorithm is presented. The controller parameters including two parts: i) the funnel parameters φ_0, φ_∞, and a; ii) the control gains $k_i, i = 1, ..., 4$ and NN parameters Γ_1, Γ_2, σ_1 and σ_2, which can be summarized as follows.

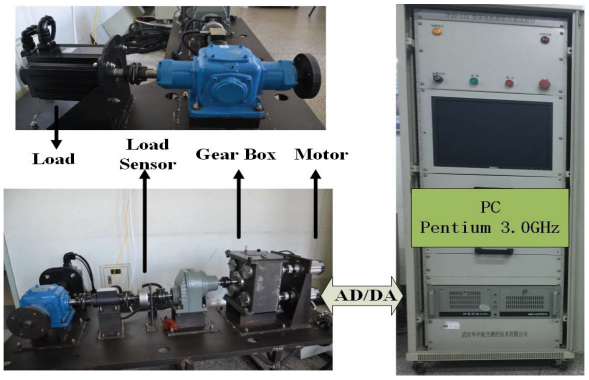

FIGURE 5. Structure of two inertia servo mechanism.

1) Select the funnel parameters φ_{0i}, $\varphi_{\infty i}$, and a_i, which should satisfy $|z_i(0)| < F_{\varphi i}(0)$.

2) The NN weights $\hat{W}_i(0), i = 1, 2$ should be nonnegative, i.e. $\hat{W}_i(0) = 0$. In addition, large σ_1 and σ_2 will suppress the parameter adaptive speed.

3) Parameter k_i can lead to fast convergence of tracking error and the control action produces oscillation. The gains i can improve the estimation performance, but may be lead to the oscillation.

IV. EXPERIMENT RESULTS

A. EXPERIMENTAL SETUP

To test the effectiveness of the developed control method, the experiment are carried out based on a two-inertia servo mechanism (See Fig.5). This control system is composed of a driving motor with the pulse width modulation (PWM) amplifier located in the driving card (Panasonic MCDDT3520), an electromotor (180ST-M 35105) with 64000 counts per rotation resolution encoder as the load, a digital signal processing (TMS320 2812) unit performing for communication, and a Pentium 3.0 GHz industrial control computer by running C++ program in CCS 5.0 developing environment. The load is driven by the driving motor through the transmission gear. The industrial computer receives the signals of the driving motor and load from the encoder, and provides the corresponding control action for real-time control. The sampling time is $ts = 0.001s$.

B. CONTROLLER DESIGN

In order to validate control performance of the developed control algorithm, three control methods are compared in this part.

1) ANFC: The adaptive neural control scheme with funnel control is performed. The funnel parameters are given as $F_{\varphi i} = \varphi_{0\,i} \cdot \exp(-a_i t) + \varphi_{\infty i}$ with $\varphi_{0\,i} = 0.12$, $\varphi_{\infty i} = 0.028$ and $a_i = 1.5 (i = 1, 2, 3, 4)$. The controller parameters are chosen as $k_1 = 2$, $k_2 = 4$, $k_3 = 8$ and $k_4 = 3$. The TD parameters are $\lambda_{1i} = 1.5$, $\lambda_{2i} = 12$, $\lambda_{3i} = 15$ and $\lambda_{4i} = 8$ $(i = 1, 2, 3, 4)$. The neural network parameters are selected as $\Gamma_1 = \Gamma_2 = 100$, and $\sigma_1 = \sigma_2 = 0.01$. The initial

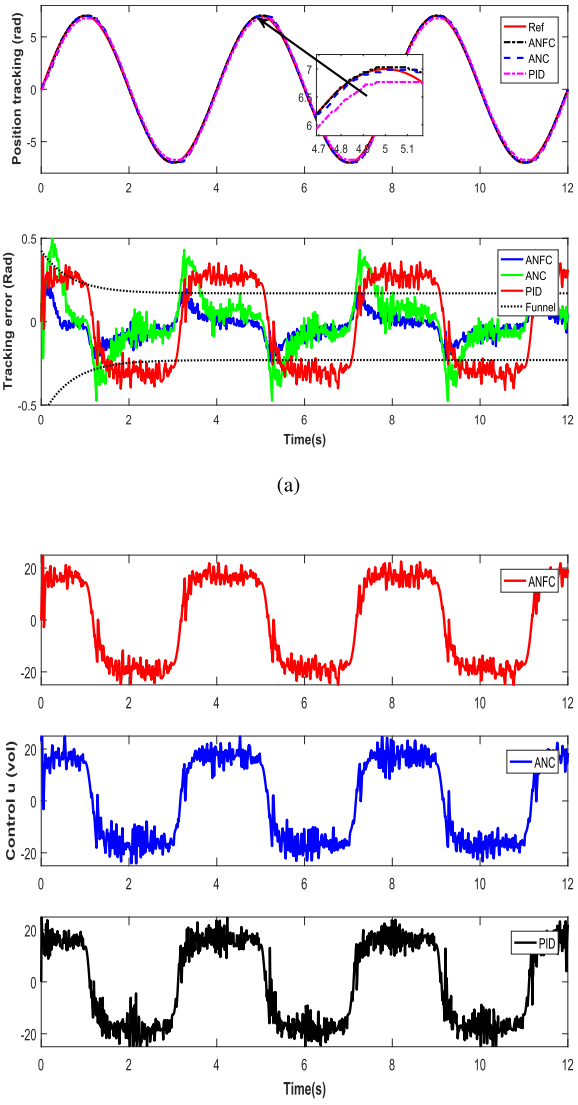

(a)

(b)

FIGURE 6. Experiment results for $x_d = 7\sin(2\pi t/4)$ (a) Position tracking and tracking errors; (b) Control u for different controllers.

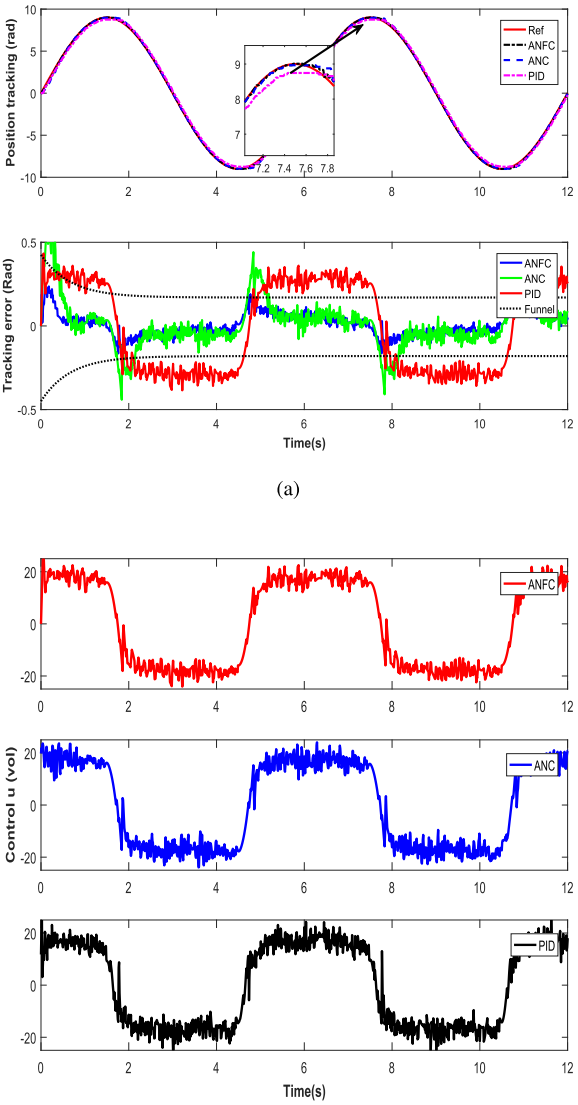

(a)

(b)

FIGURE 7. Experiment results for $x_d = 9\sin(2\pi t/6)$ (a) Position tracking and tracking errors; (b) Control u for different controllers.

weights are $\hat{W}_1(0) = \hat{W}_2(0) = 0$. The number layers of NN is $L = 6$.

2) ANC: This is an adaptive neural control without funnel control. The difference is the ANC without using the funnel function in controller design. The other control parameters and neural network parameters are the same as ANFC.

3) PID: The PID control gains are given as $k_p = 100$, $k_i = 2$ and $k_d = 10$.

C. EXPERIMENTAL RESULTS

The control performance of the developed ANFC for nonlinear servo system is experimentally evaluated by comparing their response under different position references. All the parameters are tuned to achieve the best control performance for a given reference and then fixed to validate the generality of the different controllers.

Case 1: A sinusoidal signal $x_d = 7\sin(2\pi/5)$ is employed as a desired trajectory. Fig.6 depicts the experiment result for case 1, where the position tracking performance, tracking errors (Fig.6(a)) and control action (Fig.6(b)) are all depicted. We can find from Fig.6 that the load position output can follow the reference signal x_d well by using our developed ANFC algorithm, and the tracking error of the ANFC is remained within a funnel boundary. While the tracking errors of the other two control methods (e.g., ANC and PID) exceeds the given boundary. In addition, the control action u of the proposed ANFC is smooth, nevertheless, the control action of ANC and PID produces the oscillation.

Case 2: To further compare the control performance of the designed ANFC, another sinusoidal signal $x_d = 9\sin(2\pi/6)$ with large amplitude and period is adopted. The experimental results are shown in Fig.7. As seen from these figures, the proposed ANFC performs better than ANC and PID con-

trol schemes. Compared with ANC and PID, the tracking error of the ANFC is guaranteed within prescribed boundary. This is because that the ANFC used in this paper can improve the control performance.

V. CONCLUSION

In this paper, a novel adaptive neural funnel control scheme was presented for nonlinear two-inertia servo mechanisms with backlash. A CTD was used in DSC design procedure that can improve the filter performance. The unknown dynamics are approximated by using echo state neural network and compensated in controller design. A novel funnel variable was employed and incorporated into DSC design to improve control performance. Then, an adaptive neural funnel control algorithm was developed for two-inertia servo mechanisms. The stability of the closed-loop control system was proved by using Lyapunov stability theory. Extensive comparative experiment results illustrate the benefits and reliability of the developed control algorithm in comparison to the other two algorithms.

REFERENCES

[1] S. Li and Z. Liu, "Adaptive speed control for permanent-magnet synchronous motor system with variations of load inertia," *IEEE Trans. Ind. Electron.*, vol. 56, no. 8, pp. 3050–3059, Aug. 2009.
[2] S. Wang, X. Ren, J. Na, and T. Zeng, "Extended-state-observer-based funnel control for nonlinear servomechanisms with prescribed tracking performance," *IEEE Trans. Autom. Sci. Eng.*, vol. 14, no. 1, pp. 98–108, Jan. 2017.
[3] J. Na, Q. Chen, X. Ren, and Y. Guo, "Adaptive prescribed performance motion control of servo mechanisms with friction compensation," *IEEE Trans. Ind. Electron.*, vol. 61, no. 1, pp. 486–494, Jan. 2014.
[4] Q. Chen, X. Ren, J. Na, and D. Zheng, "Adaptive robust finite-time neural control of uncertain pmsm servo system with nonlinear dead zone," *Neural Comput. Appl.*, vol. 28, no. 12, pp. 3725–3736, Dec. 2017.
[5] S. Wang, H. Yu, J. Yu, J. Na, and X. Ren, "Neural-network-based adaptive funnel control for servo mechanisms with unknown dead-zone," *IEEE Trans. Cybern.*, to be published.
[6] J. Na, S. Wang, Y. Liu, Y. Huang, and X. Ren, "Finite-time convergence adaptive neural network control for nonlinear servo systems," *IEEE Trans. Cybern.*, to be published.
[7] J. Na, Y. Li, Y. Huang, G. Gao, and Q. Chen, "Output feedback control of uncertain hydraulic servo systems," *IEEE Trans. Ind. Electron.*, to be published.
[8] S. Ding, J. Wang, and W. Zheng, "Second-order sliding mode control for nonlinear uncertain systems bounded by positive functions," *IEEE Trans. Ind. Electron.*, vol. 62, no. 9, pp. 5899–5909, Sep. 2015.
[9] Q. Chen, S. Xie, M. Sun, and X. He, "Adaptive nonsingular fixed-time attitude stabilization of uncertain spacecraft," *IEEE Trans. Aerosp. Electron. Syst.*, vol. 54, no. 6, pp. 2937–2950, Dec. 2018.
[10] Z. Li, J. Chen, G. Zhang, and M. Gan, "Adaptive robust control of servo mechanisms with compensation for nonlinearly parameterized dynamic friction," *IEEE Trans. Control Syst. Technol.*, vol. 21, no. 1, pp. 194–202, Jan. 2013.
[11] Y. Jia, "Robust control with decoupling performance for steering and traction of 4WS vehicles under velocity-varying motion," *IEEE Trans. Control Syst. Technol.*, vol. 8, no. 3, pp. 554–569, May 2000.
[12] M. Chen, S.-Y. Shao, and B. Jiang, "Adaptive neural control of uncertain nonlinear systems using disturbance observer," *IEEE Trans. Cybern.*, vol. 47, no. 10, pp. 3110–3123, Oct. 2017.
[13] Y. Zhang, G. Tao, and M. Chen, "Adaptive neural network based control of noncanonical nonlinear systems," *IEEE Trans. Neural Netw. Learn. Syst.*, vol. 27, no. 9, pp. 1864–1877, Sep. 2016.
[14] M. Chen, G. Tao, and B. Jiang, "Dynamic surface control using neural networks for a class of uncertain nonlinear systems with input saturation," *IEEE Trans. Neural Netw. Learn. Syst.*, vol. 26, no. 9, pp. 2086–2097, Sep. 2015.
[15] Q. Chen, L. Shi, J. Na, X. Ren, and Y. Nan, "Adaptive echo state network control for a class of pure-feedback systems with input and output constraints," *Neurocomputing*, vol. 275, pp. 1370–1382, Jan. 2018.
[16] T. Gao, Y.-J. Liu, L. Liu, and D. Li, "Adaptive neural network-based control for a class of nonlinear pure-feedback systems with time-varying full state constraints," *IEEE/CAA J. Autom. Sinica*, vol. 5, no. 5, pp. 923–933, Sep. 2018.
[17] D.-P. Li and D.-J. Li, "Adaptive neural tracking control for an uncertain state constrained robotic manipulator with unknown time-varying delays," *IEEE Trans. Syst., Man, Cybern., Syst.*, vol. 48, no. 12, pp. 2219–2228, Dec. 2018.
[18] J. Yu, L. Zhao, H. Yu, C. Lin, and W. Dong, "Fuzzy finite-time command filtered control of nonlinear systems with input saturation," *IEEE Trans. Cybern.*, vol. 48, no. 8, pp. 2378–2387, Aug. 2018.
[19] J. Yu, P. Shi, W. Dong, and C. Lin, "Adaptive fuzzy control of nonlinear systems with unknown dead zones based on command filtering," *IEEE Trans. Fuzzy Syst.*, vol. 26, no. 1, pp. 46–55, Feb. 2018.
[20] L. Liu, Y.-J. Liu, and S. Tong, "Fuzzy based multi-error constraint control for switched nonlinear systems and its applications," *IEEE Trans. Fuzzy Syst.*, to be published.
[21] J. Na, Y. Huang, X. Wu, S.-F. Su, and G. Li, "Adaptive finite-time fuzzy control of nonlinear active suspension systems with input delay," *IEEE Trans. Cybern.*, to be published.
[22] S. S. Ge, F. Hong, and T. H. Lee, "Adaptive neural network control of nonlinear systems with unknown time delays," *IEEE Trans. Autom. Control*, vol. 48, no. 11, pp. 2004–2010, Nov. 2003.
[23] J. Zhou, C. Wen, and Y. Zhang, "Adaptive backstepping control of a class of uncertain nonlinear systems with unknown backlash-like hysteresis," *IEEE Trans. Autom. Control*, vol. 49, no. 10, pp. 1751–1759, Oct. 2004.
[24] Z. Liu, B. Chen, and C. Lin, "Adaptive neural backstepping for a class of switched nonlinear system without strict-feedback form," *IEEE Trans. Syst., Man, Cybern., Syst.*, vol. 47, no. 7, pp. 1315–1320, Jul. 2017.
[25] D. Swaroop, J. K. Hedrick, P. P. Yip, and J. C. Gerdes, "Dynamic surface control for a class of nonlinear systems," *IEEE Trans. Autom. Control*, vol. 45, no. 10, pp. 1893–1899, Oct. 2000.
[26] B. Xu, Z. Shi, C. Yang, and F. Sun, "Composite neural dynamic surface control of a class of uncertain nonlinear systems in strict-feedback form," *IEEE Trans. Cybern.*, vol. 44, no. 12, pp. 2626–2634, Dec. 2014.
[27] Z. Peng, D. Wang, Z. Chen, X. Hu, and W. Lan, "Adaptive dynamic surface control for formations of autonomous surface vehicles with uncertain dynamics," *IEEE Trans. Control Syst. Technol.*, vol. 21, no. 2, pp. 513–520, Mar. 2013.
[28] G. Zhang, J. Chen, and Z. Lee, "Adaptive robust control for servo mechanisms with partially unknown states via dynamic surface control approach," *IEEE Trans. Control Syst. Technol.*, vol. 18, no. 3, pp. 723–731, Mar. 2010.
[29] Y. Li, S. Tong, and T. Li, "Adaptive fuzzy output feedback dynamic surface control of interconnected nonlinear pure-feedback systems," *IEEE Trans. Cybern.*, vol. 45, no. 1, pp. 138–149, Jan. 2015.
[30] J. Na, X. Ren, G. Herrmann, and Z. Qiao, "Adaptive neural dynamic surface control for servo systems with unknown dead-zone," *Control Eng. Pract.*, vol. 19, no. 11, pp. 1328–1343, 2011.
[31] G. Sun, D. Li, and X. Ren, "Modified neural dynamic surface approach to output feedback of MIMO nonlinear systems," *IEEE Trans. Neural Netw. Learn. Syst.*, vol. 26, no. 2, pp. 224–236, Feb. 2015.
[32] C. P. Bechlioulis and G. A. Rovithakis, "Robust adaptive control of feedback linearizable MIMO nonlinear systems with prescribed performance," *IEEE Trans. Autom. Control*, vol. 53, no. 9, pp. 2090–2099, Oct. 2008.
[33] S. Wang, J. Na, and X. Ren, "Rise-based asymptotic prescribed performance tracking control of nonlinear servo mechanisms," *IEEE Trans. Syst., Man, Cybern., Syst.*, vol. 48, no. 12, pp. 2359–2370, Dec. 2018.
[34] Q. Hu, X. Shao, and L. Guo, "Adaptive fault-tolerant attitude tracking control of spacecraft with prescribed performance," *IEEE/ASME Trans. Mechatronics*, vol. 23, no. 1, pp. 331–341, Feb. 2018.
[35] Y. Zhu, J. Qiao, and L. Guo, "Adaptive sliding mode disturbance observer-based composite control with prescribed performance of space manipulators for target capturing," *IEEE Trans. Ind. Electron.*, vol. 66, no. 3, pp. 1973–1983, Mar. 2019.
[36] Z. Zheng and M. Feroskhan, "Path following of a surface vessel with prescribed performance in the presence of input saturation and external disturbances," *IEEE/ASME Trans. Mechatronics*, vol. 22, no. 6, pp. 2564–2575, Dec. 2017.

[37] J. Na, Y. Huang, X. Wu, G. Gao, G. Herrmann, and J. Z. Jiang, "Active adaptive estimation and control for vehicle suspensions with prescribed performance," *IEEE Trans. Control Syst. Technol.*, vol. 26, no. 6, pp. 2063–2077, Nov. 2018.
[38] A. Ilchmann, E. P. Ryan, and P. Townsend, "Tracking control with prescribed transient behaviour for systems of known relative degree," *Syst. Control Lett.*, vol. 55, no. 5, pp. 396–406, 2006.
[39] A. Ilchmann and H. Schuster, "PI-funnel control for two mass systems," *IEEE Trans. Autom. Control*, vol. 54, no. 4, pp. 918–923, Apr. 2009.
[40] S. Wang, J. Na, X. Ren, H. Yu, and J. Yu, "Unknown input observer-based robust adaptive funnel motion control for nonlinear servomechanisms," *Int. J. Robust Nonlinear Control*, vol. 28, no. 18, pp. 6163–6179, 2018.
[41] C. M. Hackl, C. Endisch, and D. Schröder, "Contributions to non-identifier based adaptive control in mechatronics," *Robot. Auton. Syst.*, vol. 57, no. 10, pp. 996–1005, 2009.
[42] X. Wang and H. Lin, "Design and analysis of a continuous hybrid differentiator," *IET Control Theory Appl.*, vol. 5, no. 11, pp. 1321–1334, 2011.

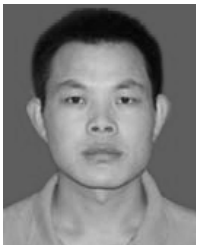

SHUBO WANG (M'19) received the B.S. degree in physics from Binzhou University, Shandong, China, in 2008, the M.S degree in control science and engineering from the School of Information Science and Engineering, Central South University, Hunan, China, in 2011, and the Ph.D. degree in control science and engineering from the Beijing Institute of Technology, Beijing, China, in 2017.

Since 2017, he has been with the School of Automation, Qingdao University. His current research interests include adaptive control, adaptive parameter estimation, neural networks, motor control, nonlinear control, and their applications.

HAISHENG YU received the B.S. degree in electrical automation from the Harbin University of Civil Engineering and Architecture, in 1985, the M.S. degree in computer applications from Tsinghua University, in 1988, and the Ph.D. degree in control science and engineering from Shandong University, China, in 2006. He is currently a Professor with the School of Automation, Qingdao University, China. His research interests include electrical energy conversion and motor control, applied nonlinear control, computer control, and intelligent systems.

JINPENG YU received the B.Sc. degree in automation from Qingdao University, Qingdao, China, in 2002, the M.Sc. degree in system engineering from Shandong University, Jinan, China, in 2006, and the Ph.D. degree from the Institute of Complexity Science, Qingdao University, in 2011, where he is currently a Distinguished Professor with the School of Automation and Electrical Engineering.

His research interests include electrical energy conversion and motor control, applied nonlinear control, and intelligent systems. He was a recipient of the Shandong Province Taishan Scholar Special Project Fund and the Shandong Province Fund for Outstanding Young Scholars.

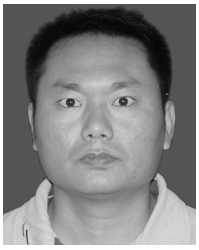

XUEHUI GAO (M'16) received the master's degree from the School of Information and Electrical Engineering, Shandong University of Science and Technology, Qingdao, China, in 2006, and the Ph.D. degree in control science and engineering from the Beijing Institute of Technology, Beijing, China, in 2016.

Since 2006, he has been with the Department of Mechanical and Electrical Engineering, Shandong University of Science and Technology, Tai'an. His current research interests include hysteresis system identification and control, adaptive control, and neural networks.